Available online at www.sciencedirect.com
SCIENCE DIRECT®
Thermochimica Acta 432 (2005) 41–46
thermochimica acta
www.elsevier.com/locate/tca

Reduced fluidity of dipalmitoyl phosphatidic acid membranes by salicylic acid

Lata Panicker [a,*], S.L. Narasimhan [a], K.P. Mishra [b]

[a] *Bhabha Atomic Research Centre, Solid State Physics Division, Mumbai 400085, India*
[b] *Radiation Biology and Health Sciences Division, Bhabha Atomic Research Centre, Mumbai 400085, India*

Received 8 September 2004; received in revised form 1 April 2005; accepted 11 April 2005

Abstract

This paper presents DSC and NMR study of how the kerotolytic drug, salicylic acid (SA), affects the thermotropic and morphological behavior of a model membrane, dipalmitoyl phosphatidic acid (DPPA). The membrane–drug system has been studied in the multilamellar vesicular (MLV) and in the unilamellar vesicular (ULV) forms, for SA/DPPA molar ratios from 0 to 0.5. The mode of interaction of SA molecules with DPPA is similar in MLV and ULV. Chain-melting transition becomes sharper and shifts to higher temperatures in the presence of the drug, implying an enhanced co-operativity of the acyl chains. NMR and DSC data indicate that the drug molecules are located in the aqueous interfacial region neighboring the lipid headgroups. The membrane becomes more rigid in the presence of the drug molecules, due to a stronger interaction between the lipid headgroups leading to reduced permeability. ULVs are destroyed by even a short equilibration at room temperature, whereas prolonged equilibration of the MLV only leads to a slightly reduced interaction between the lipid headgroups due to sequestering of the drug molecules in the interfacial aqueous region.

Keywords: DSC; NMR; DPPA; Salicylic acid; Unilamellar vesicles

1. Introduction

Biological membranes are composed of a lipid bilayer matrix in which proteins, steroids, cholesterol, sugars etc. are embedded [1–3]. Model membranes (lipid(s)–water systems) can be made to mimic biomembranes in various ways [4–9]. The properties of such model membranes, prepared with charged lipids, can be controlled by changing the external pH and/or the ionic strength of the dispersion at constant temperature [10–12]. Changes in the conformation of the hydrophobic chain, brought about by drug molecules under various conditions, can be determined.

One model membrane used to investigate the mode of action of drug molecules is dipalmitoyl phosphatidic acid (DPPA)–water [13–20]. Since DPPA (Fig. 1a) bears two ionizable groups with pk_a values 3.9 and 8.6 [21–23], the negative surface charge of this membrane can be varied and the chain-melting transition temperature, T_m, is pH-dependent [24–28]. Melting of the lipid acyl chains is related to the permeability of the membrane, a physiologically important parameter.

The drug used in the present studies is salicylic acid (SA) (Fig. 1b), a kerotolytic drug used as an antiseptic and antipruritic in the treatment of wounds and parasitic skin diseases. DSC and (^{1}H and ^{31}P) NMR study of how the presence of the drug, SA, affects the conformational phase behavior of DPPA dispersions is presented here.

2. Materials and methods

2.1. Sample preparation

Membranes were prepared from the monosodium salt of L_α DPPA, purchased from Avantipolar Lipids, USA. The

* Corresponding author. Tel.: +91 22 25592021; fax: +91 22 25505151.
E-mail address: lata@magnum.barc.ernet.in (L. Panicker).

0040-6031/$ – see front matter © 2005 Elsevier B.V. All rights reserved.
doi:10.1016/j.tca.2005.04.006

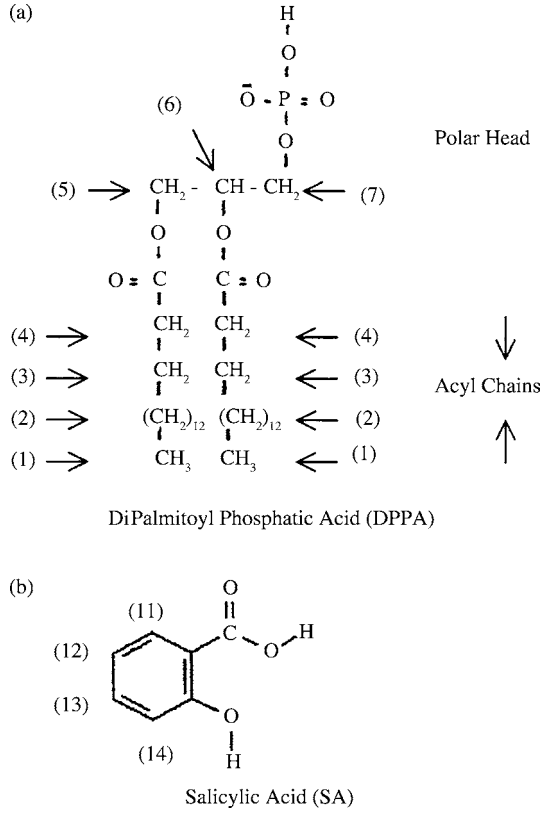

Fig. 1. Schematic structure of: (a) the phospholipid, dipalmitoyl phosphatidic acid (DPPA); and (b) the keratolytic drug, salicylic acid (SA).

drug, SA (<99% purity) was purchased from Aldrich chemical company. To prepare these membranes, a buffer of pH 9.3 was prepared with 0.05 M borax ($Na_2B_4O_7{\cdot}10H_2O$) and 0.2 M boric acid solution. The stock solution of SA was prepared in methanol, which was added to a weighed quantity of DPPA powder, so as to obtain the required molar ratio of SA to DPPA. Chloroform was then added to the mixture and mixed with a vortex mixer.

To make multilamellar vesicles (MLV) (with molar ratio, R_m in the range 0–0.5), the drug–DPPA–chloroform mixture was dried with a stream of nitrogen at room temperature, left in vacuum for at least 24 h to ensure the removal of all solvent, then hydrated with buffer. Thorough dispersion of DPPA in the buffer was achieved by heating in a water bath kept 10 °C above the chain-melting transition and then vortexing at room temperature. This procedure was repeated at least 10 times.

To obtain unilamellar vesicles (ULV) (with molar ratio in the range 0–0.3), films with the drug–lipid–chloroform mixture were formed on the inner surface of the test tube with a stream of nitrogen, left in vacuum for at least 24 h, hydrated with buffer, heated in a water bath 10 °C above the chain-melting transition temperature and vortexed at least 10 times. The mixture was then sonicated with a microtip at 10 °C above the chain-melting transition temperature (approximately 20 min), until it became translucent. The ULV was stable when prepared at pH 9.3. DPPA concentrations [DPPA] were 50 and 25 mM for DSC and NMR experiments, respectively.

Samples weighing 7–12 mg (for MLV) and 15–18 mg (for ULV) were hermetically sealed in aluminum pans for the DSC measurements. Experiments were carried out immediately (<1 h) after the respective membrane samples in MLV as well as ULV form were prepared ($\tau_e \approx 0$). Experiments were repeated again after equilibrating the samples for 1 day ($\tau_e \approx 1$ day) at room temperature, and for more than 21 days ($\tau_e > 24$ days) at room temperature. For NMR measurements, approximately 1 ml of ULV was taken in a 5 mm NMR tube.

2.2. Differential scanning calorimeter

Thermal measurements were done with Perkin-Elmer DSC-2C instrument, with an empty aluminum pan as the reference. The instrument was calibrated, using cyclohexane and indium, at a heating rate of 10 °C per minute. It was then calibrated for enthalpy at heating rates 10, 5 and 2.5 °C per minute. The chain-melting (CM) and chain ordering (CO) transitions were recorded at the same scanning speeds. The actual transition temperatures, T_m or T_{CO}, were obtained by extrapolating the values of the temperature at the peak, to zero rate. The transition enthalpy, ΔH_m, was obtained from the area under the endothermic peak in the 5 and 2.5 °C per minute scans. The full width at half maximum, Δ_m was obtained from the 5 °C per minute scans. The DSC measurements were carried out for both the MLV and the ULV membrane samples. For each value of the molar ratio, R_m, the experiment was repeated at least three times. Data were retained only for those samples in which weight loss was less than 0.2 mg, at the end of the scanning experiments.

2.3. Nuclear magnetic resonance (NMR)

Bruker AMX 500 MHz FT NMR spectrometer, fitted with a calibrated temperature control, was used for recording the spectra from ULV. D_2O and H_3PO_4 were used as references for ^1H and ^{31}P NMR experiments, respectively.

3. Results

The DSC profiles of multilamellar vesicles (MLV) obtained at a scan rate of 5 °C/min., for various molar ratios of SA to DPPA and for equilibration times, $\tau_e \approx 0$ and $\tau_e > 24$ days are shown in Fig. 2a and b, respectively. The molar ratio (R_m)-dependence of the thermotropic parameters, transition temperature, T_m, transition enthalpy, ΔH_m, and transition width (full width at half maximum), Δ_m, are shown in Fig. 3A, B and C, respectively.

The undoped-DPPA ($R_m = 0$) dispersion, when heated in the temperature range 5–70 °C, showed (Fig. 2) an endothermic chain-melting phase transition with the transition temperature, $T_m = 58.3$ °C and the associated transition enthalpy $\Delta H_m = 34.6$ kJmol^{-1} [22,29]. In SA-doped DPPA

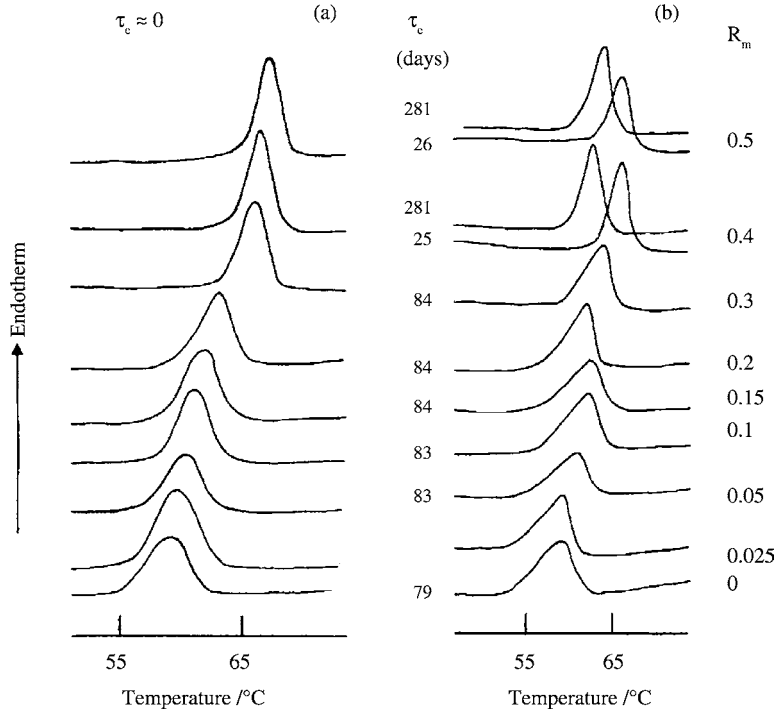

Fig. 2. The DSC heating scans at 5 °C/min of MLV for different molar ratios, R_m of SA to DPPA, and for equilibration times: (a) $\tau_e \approx 0$; and (b) τ_e, as indicated on the curve.

dispersion, the transition temperature, T_m, and the transition enthalpy, ΔH_m, increases linearly with increasing drug concentration, R_m (Fig. 3A and B). However, the transition width, Δ_m, decreases with increasing drug concentration (Fig. 3C). These observations indicate that the thermotropic properties of the DPPA bilayer are affected by the presence of the drug, SA, and this effect is concentration-dependent.

Thermotropic parameters obtained for samples equilibrated for 1 day ($\tau_e \approx 1$ day), at room temperature, did not change much as compared to their $\tau_e \approx 0$ values (Fig. 3 A–C). However, marked changes in their transition behavior, were observed after equilibrating these samples for more than 24 days ($\tau_e > 24$ days), at room temperature. At any given drug concentration, the transition temperature (Fig. 3A) is less than its value for $\tau_e \approx 0$ and 1 day, whereas the transition width (Fig. 3C) is more than its value for $\tau_e \approx 0$ and 1 day. Similar behavior is observed for the transition enthalpies (Fig. 3B). These observations suggest that prolonged equilibration results in a reduced drug–lipid interaction due to the drug molecules getting sequestered out into the lipid–water interfacial region, over a period of time.

The DSC measurements were also carried out with unilamellar vesicles (ULV) of DPPA both in presence and absence of SA. Fig. 4 gives the DSC profiles, of the ULV obtained at a scan rate of 5 °C/min, for various drug concentrations (R_m) and for $\tau_e \approx 0$. The drug concentration (R_m)-dependence of the thermotropic parameters, are shown in Fig. 3 A–C.

The DSC scan of DPPA dispersion (Fig. 4, $R_m = 0$) shows an endothermic chain-melting transition at a temperature, 53.2 °C and the associated transition enthalpy was 21.3 kJmol^{-1}. However, these values are smaller than the corresponding ones for the membrane in the MLV form. This could be due to the reduced headgroup–headgroup interaction in the ULV form, which leads to a less tight packing of the chains than in the MLV form. It may be noted, however, that the width of the transition is hardly affected by the change in the morphological structure of the membrane.

It is seen from Figs. 3 and 4 that in drug-doped-DPPA dispersion, the transition becomes sharper and occurs at higher temperatures. But, in contrast to the MLV the transition enthalpy increases dramatically (Fig. 3B,d), for $0 \leq R_m \leq 0.1$. This could probably be indicative of the fact that the drug molecule can affect the shape and size of the ULV. Besides contributing to an increase in the PA–PA head group interaction by being in the vicinity of the polar head group region, the drug molecules bring about a morphological change as well. In fact, morphological changes, rather than the increased PA–PA interaction could be the reason for the observed dramatic increase in the transition enthalpy.

Equilibration had a more pronounced effect on ULV. For example, no transition was observed for, $\tau_e \geq 1$ day for both drug-free and drug-doped membranes. It implies that equilibration destroyed the ULV. Sample tube containing ULV dispersion, when observed at $\tau_e \geq 1$ day, showed solid particles to settling at the bottom of the tube, indicating that phase separation could have taken place. It is known that the ULV are unstable below its CM transition temperature [30].

^{1}H NMR experiments were carried out with SA-doped and undoped unilamellar vesicles of DPPA. Presented in Fig. 5a are the ^{1}H NMR spectra obtained from DPPA dispersions

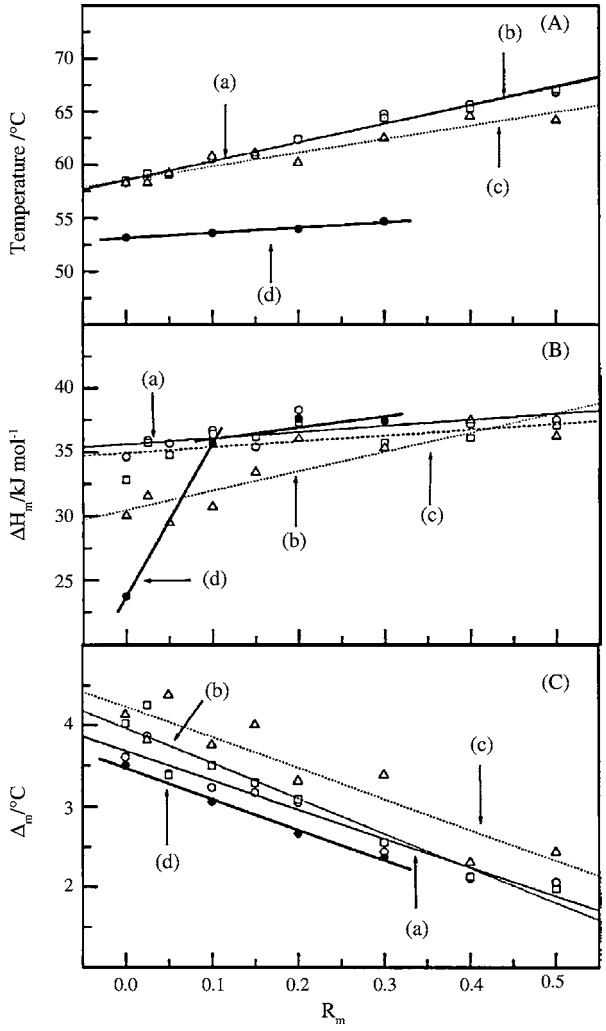

Fig. 3. R_m-dependence of transition: (A) temperature, T_m; (B) enthalpy, ΔH_m; and (C) width, Δ_m for MLV: (a) $\tau_e \approx 0$; (b) $\tau_e \approx 1$ day; and (c) $\tau_e > 24$ days and for ULV; (d) $\tau_e \approx 0$.

for various temperatures in the vicinity of the chain-melting transition temperature, T_m. Various proton resonances in the spectra can be identified with the assignments given in Fig. 1a. These spectra can be compared with those (Fig. 5b) obtained for the SA-incorporated DPPA dispersions. It is observed that the resonances, labelled 1 and 2, became sharper and better resolved as the temperature approaches T_m. The sharpening of the chain proton resonances is indicative of greater mobility of the concerned proton due to increased chain disorder. The proton resonances in the drug-doped DPPA dispersion (Fig. 5b) are broader than those in the drug-free DPPA dispersion (Fig. 5a). However, drug doping did not change the chemical shifts of the various lipidic resonances.

Fig. 6a shows ^{1}H NMR spectra of the aromatic protons, labelled 11–14, from SA (Fig. 1a) in the aqueous medium, SA-buffer at various temperatures. These spectra when compared with the spectra (Fig. 6b) of the aromatic protons obtained from DPPA–SA dispersions at various temperatures around T_m did not show any significant change in the fine structure of

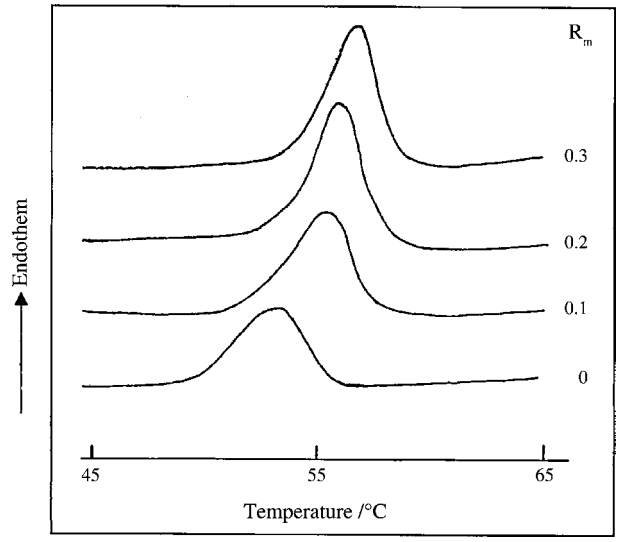

Fig. 4. DSC heating scans at 5 °C/min of ULV ([DPPA] = 50 mM), with equilibration time, $\tau_e \approx 0$. The molar ratios, R_m of SA to DPPA, are indicated on the curves.

the various aromatic proton resonances. However, the value of the chemical shift of various aromatic protons, decreased by the presence of the lipid environment. This effect could be due to the interaction of the polar groups of the drug molecules with the polar groups of the lipid or water. This interaction does not affect the aromatic proton dynamics.

^{31}P NMR measurements were carried out with SA-doped and SA-free unilamellar vesicles of DPPA, to see whether the polar group of SA interacted with the phosphate group of DPPA. ^{31}P NMR spectra from the drug-doped DPPA dispersions are presented in Fig. 7 (the spectra similar for the drug-free dispersion). Below the chain-melting transition temperature T_m, the ^{31}P resonance in either case is quite broad (powder pattern) without featuring much of the isotropic lines. It implies reduced mobility for the headgroups due to increased interaction between them in the gel phase. On the other hand, only isotropic lines are observed in the liquid crystalline phase, which resemble that of a typical ^{31}P NMR spectra of smaller unilamellar vesicles.

No significant change in the ^{31}P NMR resonance pattern is observed except that the resonance lines become sharper at higher temperatures (≈2 and 5 °C for 25 and 50 mM DPPA concentration, respectively) in the presence of the drug. This implies that the drug: (a) is located in the neighborhood of the headgroups; and (b) should be responsible for the strong headgroup–headgroup interaction.

4. Discussion

The DSC results of ULV and MLV indicate that the effect of the drug on the DPPA bilayer was more or less the same in both forms. However, for a given concentration of drug, the interaction of SA molecule with DPPA molecules is less in ULV form than in MLV form. This is because of the large

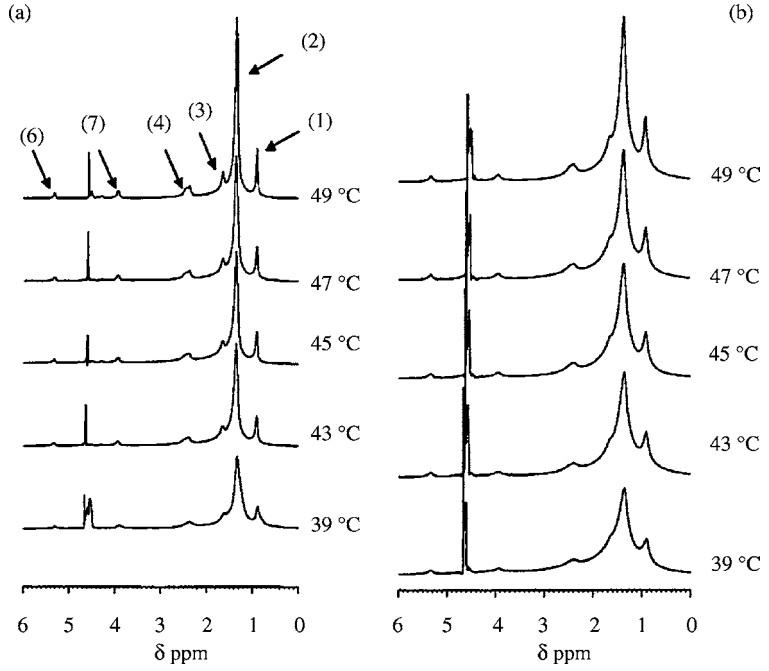

Fig. 5. ^{1}H NMR spectra of: (a) DPPA ($R_m = 0$); and (b) DPPA–SA ($R_m = 0.2$) dispersions in the vicinity of T_m ([DPPA] = 25 mM).

curvature of the ULV, which reduces the headgroup–headgroup interaction between the neighboring DPPA molecules and the larger expanse of the aqueous region available. The observed decrease in the width of the transition in response to increasing drug concentration implies that the drug molecules play definite role in bringing about increased co-operativity between the acyl chains. The increased T_m value and ^{31}P NMR spectra of the SA-doped DPPA bilayer suggest that the presence of the drug increases the headgroup–headgroup interaction of the neighboring DPPA molecules. So the presence of SA reduces membrane fluidity. Since SA is polar in nature, it is more likely to be present in the interfacial aqueous region than in the acyl-chain region (hydrophobic). This is supported by the observations that: (a) the transition enthalpy, ΔH_m, changes only slightly, from 35.6 to 37.6 kJmol^{-1}, over the drug concentration range studied in MLV; and (b) the presence of SA does not change the values of the chemical shift of the various DPPA proton resonances

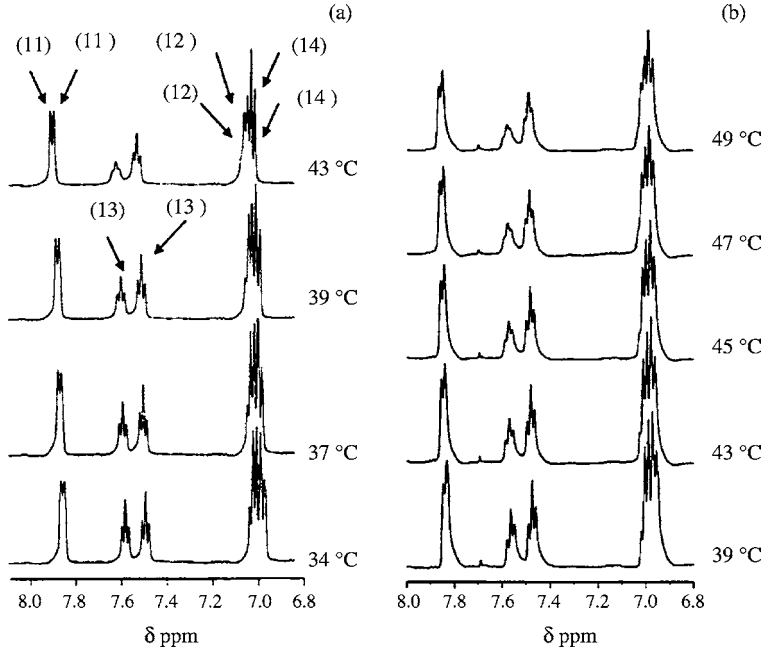

Fig. 6. Aromatic proton resonances of SA in: (a) SA-buffer; and (b) DPPA–SA ($R_m = 0.2$) dispersions, as a function of temperature.

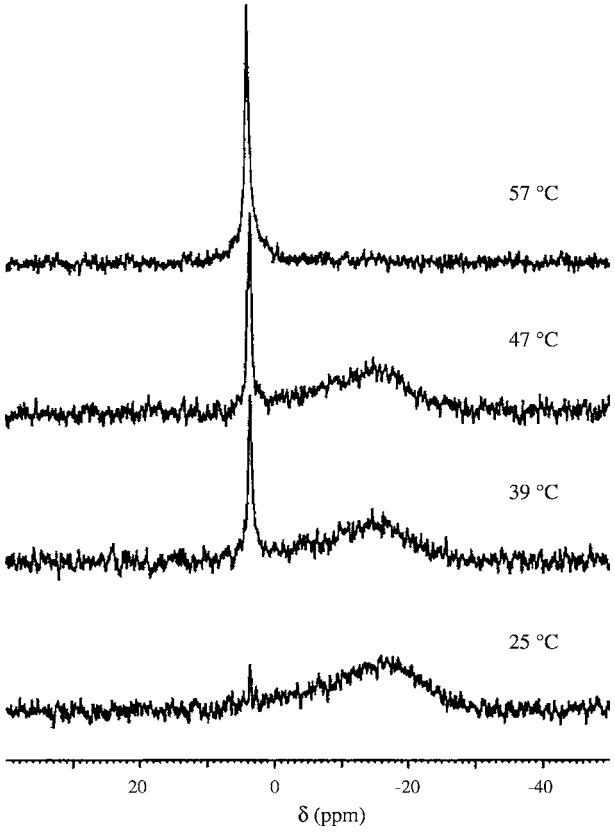

Fig. 7. ^{31}P NMR spectra of DPPA–SA dispersions in the vicinity of T_m ([DPPA] = 25 mM).

in ULV. However, in SA-doped ULV, the transition enthalpy increases dramatically, probably due to: (a) the increase in the size of the ULV or formation of vesicles with a few lamellae; and (b) the enhancement in the headgroup–headgroup interaction. The broadening of the proton resonances of DPPA acyl-chain in presence of SA also indicates that the drug increases the order (rigidity) of the acyl chains. Prolonged equilibration of MLV results in reduced drug–lipid interaction due to the drug molecules getting sequestered out into the lipid–water interfacial region over a period of time. However, equilibration leads to the destruction of the ULV itself.

The results clearly indicate that: (i) SA strongly interacts with DPPA bilayer; (ii) the drug molecules are located in the aqueous interfacial region neighboring the polar groups of the phospholipids or water molecules; and (iii) the drug molecules are responsible for increased PA–PA headgroup interaction. This leads to a better packing of the lipid chains and consequently the membrane becomes more rigid and less permeable.

References

[1] Y. Boulig (Ed.), Liquid Crystalline Order in Polymers, Blumstein Academic Press, New York, 1978.
[2] H. Hauser, G. Poupartm, in: P. Yeagle (Ed.), The Structure of Biological Membranes, CRC Press, London, 1992.
[3] M.K. Jain, R.C. Wagner (Eds.), Introduction to Biological Membranes, John Wiley, New York, 1988.
[4] R.B. Gennis (Ed.), Biomembranes: Molecular Structure and Function, Springer, New York, 1989.
[5] D. Paphadjapoulous, in: G.B. Ansell, R.M.C. Dawson, J.N. Hawthorne (Eds.), Form and Function of Phospholipids, Elsevier SPC, New York, 1973, pp. 143–169.
[6] M. Bloom, E. Evans, O.G. Mouritsen, Q. Rev. Biophys. 24 (1991) 293–397.
[7] R. Lipowsky, E. Sackmann, Structure Dynamics of Membranes. Handbook of Biological Physics, vol. 1A $\&$ B, Elsevier, Amsterdam, 1995.
[8] A. Baszkin, W. Norde (Ed.), Physical Chemistry of Biological Interfaces, Marcel Dekker, New York, 2000.
[9] D. Paphadjapoulous, in: Ostro Marc.J. (Ed.), Liposomes, Marcel Dekker, New York, 1983, pp. 241–289.
[10] F. Jahnig, K. Harlos, H. Vogel, H. Eibl, Am. Chem. Soc. 18 (1979) 1459–1468.
[11] K. Harlos, J. Stümpel, H. Eibl, Biochim. Biophys. Acta 555 (1979) 409–416.
[12] H. Eibl, A. Blume, Biochim. Biophys. Acta 553 (1979) 476–488.
[13] C. La Rosa, D. Grasso, M. Fresta, C. Ventura, G. Puglisi, Thermochim. Acta 195 (1992) 139–148.
[14] G.H. Lyman, D. Papahadjopoulos, H.D. Preisler, Biochim. Biophys. Acta 448 (1976) 460–473.
[15] E. Bernard, J. Francois Faucon, J. Dufourcq, Biochim. Biophys. Acta 688 (1982) 152–162.
[16] A. Bertoluzza, S. Bonora, G. Fini, O. Francioso, M.A. Morelli, Chem. Phys. Lipids 75 (1995) 137–143.
[17] K. Borchardt, D. Heber, M. Klingm, K. Mohr, B. Müller, Biochem. Pharmacol. 42 (1991) 561–565.
[18] H. Takahashi, S. Matuoka, S. Kato, K. Ohki, I. Hatta Biochim. Biophys. Acta 1069 (1991) 229–234.
[19] T. Cserhati, M. Szogyi, Int. J. Biochem. 23 (1991) 131–145.
[20] T. Pott, J.-C. Maillet, C. Abad, A. Campos, J. Dufourcq, E.J. Dufourc, Chem. Phys. Lipids 109 (2001) 209–223.
[21] P.W.M. van Dijck, B. de Kruijff, A.J. Verkleij, L.L.M. van Deenen, J. de Gier, Biochim. Biophys. Acta 512 (1978) 84–96.
[22] J. Minones Jr., J.M. Rodríguez Patino, J. Miñones, P. Dynarowicz-Latka, C. Carrera, J. Colloid Interface. Sci. 249 (2002) 388–397.
[23] A. Blume, Biochemistry 22 (1983) 5436–5442.
[24] R.A. Demel, C.C. Yin, B.Z. Lin, H. Hauser, Chem. Phys. Lipids 60 (1992) 209–223.
[25] H. Trauble, H. Eibl, Proc. Natl. Acad. Sci. U.S.A 71 (1974) 214–219.
[26] A. Blume, H. Eibl, Biochim. Biophys. Acta 558 (1979) 13–21.
[27] A.J. Verkleij, Biochim. Biophys. Acta 779 (1984) 43–63.
[28] A. Blume, J. Tuchtenhagen, Biochemistry 31 (1992) 4636–4642.
[29] K. Jacobson, D. Papahadjopoulos, Biochemistry 14 (1975) 152–161.
[30] B.Z. Lin, C.C. Yin, H. Hauser, Biochim. Biophys. Acta 1147 (1993) 237–244.